

Breast Tissue Characterization by Sound Speed: Correlation with Mammograms using a 2D/3D Image Registration

Torsten Hopp, Nicole V. Ruiter
Karlsruhe Institute of Technology
Institute for Data Processing and Electronics
Karlsruhe, Germany
Email: torsten.hopp@kit.edu

Neb Duric
Delphinus Medical Technologies, Inc.
Plymouth, MI, USA
Email: duric@karmanos.org

Abstract—Ultrasound Computer Tomography (USCT) is an upcoming modality for early breast cancer diagnosis, which provides morphological as well as quantitative imaging. In order to compare USCT images to the standard modality X-ray mammography, a 2D/3D registration has to be applied. To analyze the relevance of sound speed images as a quantitative imaging method for tissue characterization, the aim of this paper is to quantify sound speed values of different types of tissue using mammograms as ground truth. Mammograms are segmented and classified into fat, glandular and tumorous tissue. For each tissue class the average sound speed in the registered sound speed image is calculated. The mean absolute sound speed was 1457 m/s for regions segmented as fatty tissue, 1470 m/s for glandular and 1509 m/s for tumorous tissue. For all ten datasets, the sound speed in tumorous tissue was significantly higher than in glandular and fatty tissue. Also glandular and fatty tissue could be separated easily by the absolute sound speed values. By color-coding sound speed, quantitative information from USCT and morphological information from X-ray mammography are fused for combined diagnosis. We believe this method will help radiologists in gaining experience in the reading of USCT images. The combination of diagnostic information is likely to be beneficial to early breast cancer detection.

I. INTRODUCTION

Ultrasound Computer Tomography (USCT) [1][2] is an upcoming modality for early breast cancer detection. It offers three-dimensional volume imaging of the breast in prone position. The image acquisition is based on numerous ultrasound transducers, which surround the breast within a water bath. From the acquired signal data, it is possible to reconstruct three types of images: reflection images, attenuation images and sound speed images. Reflection images reveal changes in the echo texture resulting in imaging of the surfaces of different tissues. Attenuation and especially sound speed images are expected to provide a quantitative tissue characterization [3].

Since USCT is still in development, comparison of these images with the standard screening method mammography is of high interest. X-ray mammograms image the patient in upright position with the breast compressed between parallel plates to enhance the contrast of the images. 2D projection images are acquired. Due to the difference in dimensionality

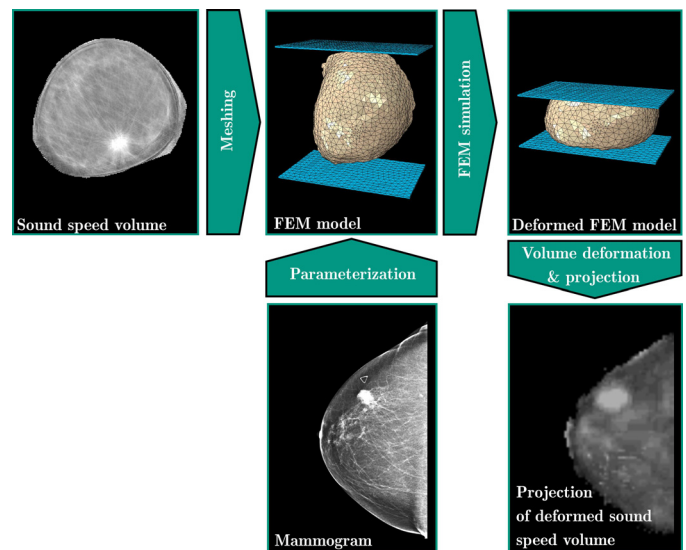


Fig. 1. Simplified principle of the registration process. A FEM model is created based on the segmented sound speed volume using a meshing algorithm. The model is parameterized by information from the mammogram. Afterwards the compression simulation is carried out. Based on the resulting deformed FEM model, the USCT volume is deformed and projected, creating an image directly comparable to the mammogram.

and compression state of the breast between X-ray mammography and USCT, the correlation of both imaging methods is challenging. To overcome this challenge, we developed an automatic 2D/3D registration method in our previous work [4][5]. It is based on a patient-specific biomechanical model to simulate the huge deformation which is applied to the breast during mammography (Figure 1). The model is described by the Finite Element Method (FEM) and built up based on the volume image. The FEM simulation then mimics the mammographic compression resulting in a similar configuration of the volume image as in the corresponding mammogram. The projection of the deformed volume image has overlaying circumferences with the mammogram. Hence, both modalities can be compared directly.

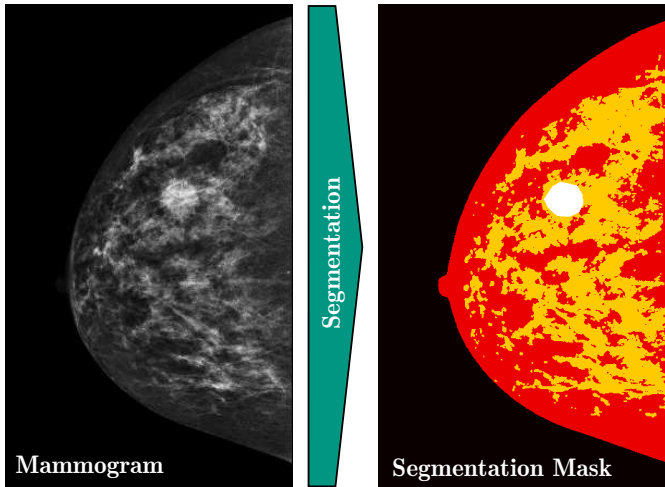


Fig. 2. Original mammogram (left) and segmentation mask (right). The colors indicate the segmented three types of tissue within the breast: fatty tissue (red), glandular tissue (yellow) and lesion (white).

The method was used in previous work to carry out an image fusion of sound speed volumes with X-ray mammograms [6][7]. The fusion of diagnostic information may benefit combined reading in radiological diagnosis. Especially for dense breast tissue, in which the sensitivity of X-ray mammography is limited [8], characterization by quantitative imaging like sound speed may provide a guidance for diagnosis of cancerous lesions. To analyze the relevance of sound speed as quantitative measure for tissue characterization, the aim of this paper is to quantify sound speed values of different types of tissue using mammograms as ground truth.

II. METHODS

In order to compare morphological structures in X-ray mammograms with the quantitative values in sound speed images, different types of tissue in the X-ray mammogram were segmented. Fatty and fibroglandular tissue were differentiated using an interactive thresholding method similar to [9]. Tumors were manually annotated by an expert using a freehand tool. A resulting segmentation mask is illustrated in Fig. 2. For evaluation purposes, only datasets with clearly visible lesions in the X-ray mammograms as well as in the sound speed images were included.

Sound speed images of the corresponding patient were acquired within a clinical study using an experimental USCT device at Karmanos Cancer Institute (KCI), Detroit, USA [10]. It consists of a ring-shaped aperture with 256 ultrasound transducers embedded in a water basin. The aperture can be translated in steps of 1 mm to acquire multiple slice images of the breast. The images have an in-plane resolution of 1 mm. Due to a focusing in elevation direction, one slice integrates over a height of 4 mm. The number of slices as well as the distance between the slices varies depending on the size of the patient's breast. The images are segmented into background and object using an automatic segmentation algorithm provided by KCI. Afterwards a scaling and rotation is applied

to fit the orientation of the mammogram. An interpolation is carried out to overcome the possible gap between the slices.

The preprocessed sound speed volume images are registered to the X-ray mammogram using our automated 2D/3D registration method based on biomechanical compression simulation as described in [6]. The geometry of the biomechanical model is specified by a hexahedral mesh which is built up based on the sound speed volume image using a transfinite interpolation algorithm [11]. The physical behavior is defined by applying a material model and boundary conditions. The breast is assumed to be nearly incompressible, i.e. the Poisson's ratio is near 0.5. The stress-strain relationship is defined by a hyper-elastic neo-hookean material model. A homogeneous material mimicking fatty tissue is used for the entire breast. Inner structures of the breast are not considered due to experiments stating that there is no major effect in using a more complex model [4]. The mammographic compression is mimicked by a two step approach. In the first step, compression plates are added to the simulation. The deformation is carried out by moving the plate until a defined compression thickness is reached. Due to simplifications and uncertainties in this process, images do not overlap congruently after carrying out the first simulation step. Therefore in the second step, the shape of this deformed breast is refined to meet the circumferences of the corresponding mammogram by node displacements. The numerical solution of all compression simulations is based on FEM and was computed using Ansys [12].

After the registration process, a maximum intensity projection of the registered sound speed volume was created, i.e. the highest sound speed value in projection direction was obtained. Due to the registration process, the resulting projection overlaps with the corresponding X-ray mammogram. This enables to correlate the segmentation mask of the X-ray mammogram with the sound speed values and therefore to quantify sound speed characteristics of different types of tissue. For each segmented tissue type in the X-ray mammogram, the sound speed values at the corresponding area in the sound speed projection image were analyzed and the mean respectively median sound speed value for each tissue category in each dataset was calculated. Descriptive statistics was used to obtain quantitative results.

Afterwards sound speed overlay images were created for visualization. Sound speed values in the maximum intensity projection image are color coded and upsampled to the resolution of the X-ray mammogram using a linear interpolation. Finally they are rendered semi-transparently on the gray level X-ray mammogram.

III. RESULTS

The evaluation of the presented method was carried out with ten clinical datasets. Each dataset consists of a sound speed volume and the corresponding cranio-caudal mammogram. Lesion positions were annotated by an expert in both modalities. The target registration error (TRE) was calculated by measuring the displacement of the center of these annotations

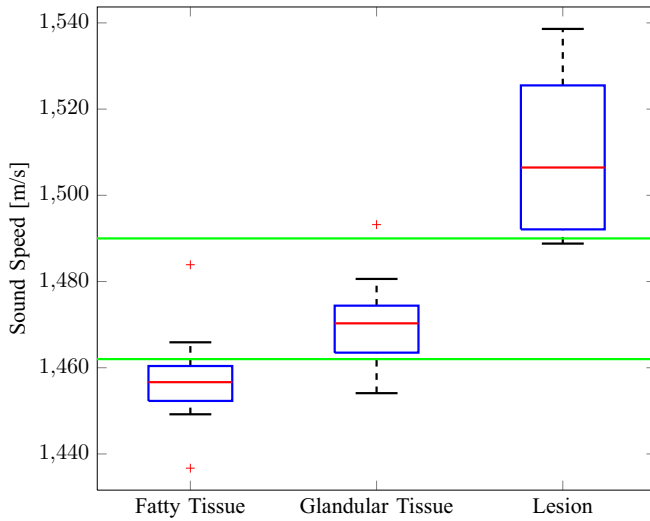


Fig. 3. Box plot of mean sound speed values for different types of tissue. The green horizontal lines give the thresholds to distinguish fatty from glandular respectively glandular from tumorous tissue, which was calculated by maximization of the inter-class variance.

in the projection image. After carrying out the registration for all ten datasets, the mean TRE was 8.4 mm (± 6.0 mm).

In the next step, sound speed values in the projection images were analyzed. The average over all the mean absolute sound speed values for each dataset was 1457 m/s (± 12 m/s) for regions segmented as fatty tissue, 1470 m/s (± 12 m/s) for fibroglandular and 1509 m/s (± 18 m/s) for tumorous tissue. The observed values are illustrated as boxplot in Fig. 3.

Statistical significance was tested using a t-Test. The differences of absolute sound speeds between fatty and glandular tissue ($p < 0.03$) respectively glandular and tumorous tissue ($p < 0.001$) are statistically significant.

In order to account for biasing of these results by e.g. interpolation artifacts, the median absolute sound speed was calculated for each region segmented in the mammogram. The average over all ten datasets was 1457 m/s (± 12 m/s) for fatty tissue, 1465 m/s (± 12 m/s) for fibroglandular tissue and 1510 m/s (± 20 m/s) for tumorous tissue respectively. Although the values for fatty and glandular tissue are closer, the tumorous tissue can be distinguished from healthy tissue very well since the standard deviations do not overlap. In all cases, glandular tissue shows a higher sound speed than fatty tissue and the lesion shows a higher sound speed than glandular tissue.

After analysis, the sound speed information were fused with the mammograms using the method described in section II. The threshold between each two types of tissue was calculated by maximizing the inter-class variance according to the Otsu method [13]. The threshold to distinguish fatty from glandular tissue was 1462 m/s, to distinguish glandular from tumorous tissue 1490 m/s (green line in Fig 3). Fatty, glandular and tumorous tissue can be highlighted in the X-ray mammograms by applying these sound speed windows to the projection

image. Two examples are shown in Fig. 4.

IV. DISCUSSION AND CONCLUSION

In this paper we presented an evaluation of sound speed volumes acquired by Ultrasound Computer Tomography for the purpose of tissue characterization. The registration of sound speed volume images with X-ray mammogram enables direct comparison of two-dimensional morphological imaging with quantitative three-dimensional imaging. By segmenting the X-ray mammograms we were able to quantify mean sound speed values for different types of tissue depicted in X-ray mammography.

Though a relatively small patient collective with obvious lesions was included in this study, the obtained results are promising. In all cases, the lesions had a significantly increased sound speed in the projection image compared to surrounding tissue. Also glandular and fatty tissue could be separated well by the absolute sound speed values. The results are limited by the registration accuracy, since a misregistration of tissue structures results in blurring on the obtained values at corresponding image regions. Yet, by color-coding sound speed values, the thereby highlighted tissue structures tend to clearly follow the tissue structures in the mammogram. Our current work focuses on the evaluation with a higher number of datasets to increase statistical robustness. In a next step, a clinical study may investigate the diagnostic impact of our image fusion method.

To the best of our knowledge, a quantitative analysis of sound speed in correlation with the different types of tissue depicted in X-ray mammograms has not been carried out before. Quantitative information from sound speed volume images may now be used in combination with mammography for multimodal diagnosis. We believe this method will help radiologists in gaining experience in the reading of USCT images. It is likely to be beneficial to early breast cancer detection.

REFERENCES

- [1] N. Duric, P. Littrup, L. Poulou, A. Babkin, R. Pevzner, E. Holsapple, O. Rama, and C. Glide, "Detection of Breast Cancer with Ultrasound Tomography: First Results with the Computerized Ultrasound Risk Evaluation (C.U.R.E)," *Medical Physics*, vol. 34, no. 2, pp. 773–785, 2007.
- [2] H. Gemmeke and N. Ruiter, "3D Ultrasound Computer Tomography for Medical Imaging," *Nuclear Instruments and Methods in Physics Research Section A: Accelerators, Spectrometers, Detectors and Associated Equipment*, vol. 580, no. 2, pp. 1057 – 1065, 2007.
- [3] J. F. Greenleaf and R. C. Bahn, "Cinical Imaging with Transmissive Ultrasonic Computerized Tomography," *IEEE Transactions on Biomedical Engineering*, vol. BME-28, no. 2, pp. 177–185, 1981.
- [4] N. V. Ruiter, R. Stotzka, T. O. Mueller, H. Gemmeke, J. R. Reichenbach, and W. A. Kaiser, "Model-Based Registration of X-ray Mammograms and MR Images of the Female Breast," *IEEE Transactions on Nuclear Science*, vol. 53, no. 1, pp. 204–211, 2006.
- [5] T. Hopp, "Multimodal Registration of X-Ray Mammograms with 3D Volume Datasets," Ph.D. dissertation, University of Mannheim, 2012.
- [6] T. Hopp, M. Holzapfel, N. V. Ruiter, C. Li, and N. Duric, "Registration of X-ray Mammograms and Three-Dimensional Speed of Sound Images of the Female Breast," in *Proceedings SPIE Medical Imaging*, vol. 7629, no. 1, 2010, p. 762905.

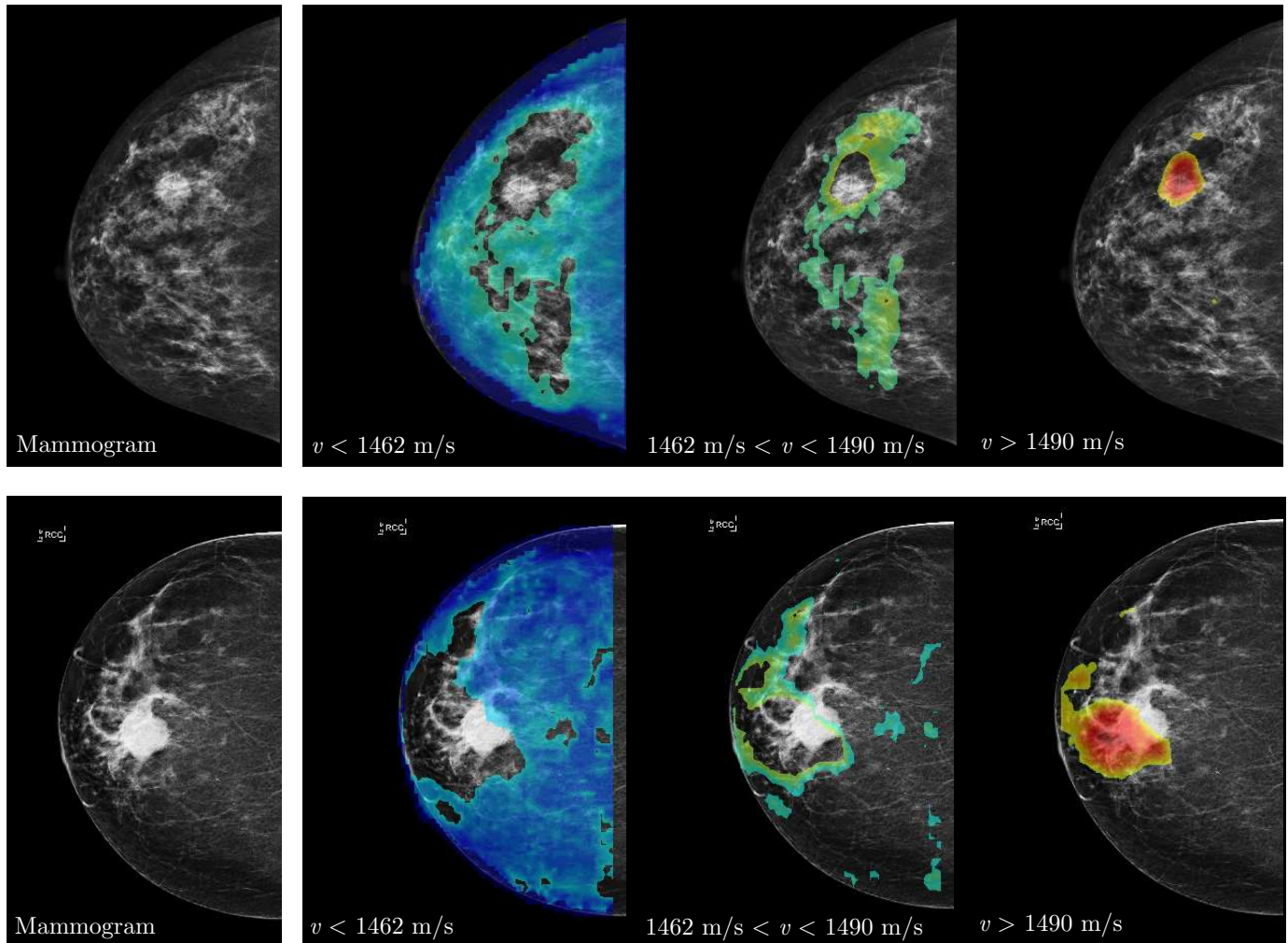


Fig. 4. Semi-transparent overlay of sound speed information on the X-ray mammogram. Thresholds on the sound speed v have been set according to the calculated values to highlight fatty (predominantly blue), fibroglandular (predominantly green) and tumor tissue (predominantly red). The upper case depicts a scattered dense breast while the lower case shows a fatty breast with only few glandular structures. The offset between the lesion in the mammogram and the overlay appears due to the registration error.

- [7] T. Hopp, J. Bonn, N. V. Ruiter, M. Sak, and N. Duric, "2D/3D Image Fusion of X-ray Mammograms with Speed of Sound Images: Evaluation and Visualization," in *Proceedings SPIE Medical Imaging*, vol. 7968, no. 1, 2011, p. 79680L.
- [8] E. D. Pisano, R. E. Hendrick, M. J. Yaffe, J. K. Baum, S. Acharyya, J. B. Cormack, L. A. Hanna, E. F. Conant, L. L. Fajardo, L. W. Bassett, C. J. D'Orsi, R. A. Jong, M. Rebner, A. N. A. Tosteson, and C. A. Gatsonis, "Diagnostic Accuracy of Digital Versus Film Mammography: Exploratory Analysis of Selected Population Subgroups in DMIST1," *Radiology*, vol. 246, no. 2, pp. 376–383, 2008.
- [9] J. W. Byng, N. F. Boyd, E. Fishell, R. A. Jong, and M. J. Yaffe, "The quantitative analysis of mammographic densities," *Physics in Medicine and Biology*, vol. 39, no. 10, p. 1629, 1994.
- [10] N. Duric, P. Littrup, P. Chandiwalla-Mody, C. Li, S. Schmidt, L. Myc, O. Rama, L. Bey-Knight, J. Lupinacci, B. Ranger, A. Szczepanski, and E. West, "In-Vivo Imaging Results with Ultrasound Tomography: Report on an Ongoing Study at the Karmanos Cancer Institute," in *Proceedings SPIE Medical Imaging*, vol. 7629, no. 1, 2010, p. 76290M.
- [11] P. Knupp and S. Steinberg, *Fundamentals of Grid Generation*. CRC Press, 1994.
- [12] ANSYS Inc. Software Products. [Online]. Available: <http://www.ansys.com>
- [13] N. Otsu, "A Threshold Selection Method from Gray-Level Histograms," *IEEE Transactions on Systems, Man and Cybernetics*, vol. 9, no. 1, pp. 62–66, 1979.